Hindawi
Mathematical Problems in Engineering
Volume 2022, Article ID 1133575, 12 pages
https://doi.org/10.1155/2022/1133575

Research Article

Pixel-Boundary-Dependent Segmentation Method for Early Detection of Diabetic Retinopathy

S. G. Sandhya,[1] **A. Suhasini**,[1] **and Yu-Chen Hu**[2]

[1]*Department of Computer Science and Engineering, Annamalai University, Chidambaram, Tamil Nadu, India*
[2]*Department of Computer Science and Information Management, Providence University, Taichung, Taiwan*

Correspondence should be addressed to Yu-Chen Hu; ychu@pu.edu.tw

Received 4 September 2022; Accepted 6 October 2022; Published 26 October 2022

Academic Editor: Jude Hemanth

Early and precise detection of diabetic retinopathy prevents vision impairments through computer-aided clinical procedures. Identifying the symptoms and processing those by using sophisticated clinical procedures reduces hemorrhage kind of risks. The input diabetic retinopathy images are influenced by using computer vision-based processes for segmentation and classification through feature extractions. In this article, a delimiting segmentation using knowledge learning (DS-KL) is introduced for classifying and detecting exudate regions by using varying histograms. The input image is identified for its histogram changes from the feature-dependent segmentation process. Depending on the training knowledge from multiple inputs with different exudate regions, the segmentation is performed. This segmentation identifies infected and noninfected regions across the delimiting pixel boundaries. The knowledge-learning process stores the newly identified exudate region for training and pixel correlation. The recurrent training improves the segmentation accuracy with precise detection and limited errors.

1. Introduction

Diabetic retinopathy (DR) is an eye disease that is caused due to high sugar levels or diabetes. Diabetic retinopathy affects the retina and leads to sight loss or vision loss. Diabetic retinopathy blocks the blood vessels that carry blood to the retina, which causes damage to diabetic patients. Diabetic retinopathy detection process is a complicated task to perform in an application [1]. Image segmentation is a process that segments digital images into multiple images. Image segmentation is also known as image objects or an image region mainly used for detection and recognition. Image segmentation is used in the DR detection process, which increases the accuracy rate in the detection process [2]. The contrast-limited adaptive histogram equalization (CLAHE) method is used in the DR detection process. CLAHE is mainly used to reduce the unnecessary region rates from an image which reduces the time consumption rate of the detection process. CLAHE increases the accuracy rate in the detection process, which provides necessary information for the diagnosis process. The convolutional neural network (CNN) algorithm is also used in the DR detection process that implements the image segmentation process. The feature extraction method in CNN identifies the important features extracted from the image segmentation process [3, 4].

Machine learning (ML) techniques are widely used in various applications for detection and recognition. ML techniques maximize the accuracy rate in the detection process, enhancing the system's efficiency and feasibility [5]. ML techniques are commonly used in DR detection and segmentation processes. The artificial neural network (ANN) algorithm is mostly used for the DR image segmentation process. ANN reduces the complexity and error rate in the detection process, which improves the effectiveness of the DR detection process [6]. Classification and optimization methods are used in ANN to find the important and actual regions from given images. The classification process classifies the data based on certain features and patterns. The support vector machine (SVM) approach is also used in segmentation processes that find out the exact segments of an image. Diabetic retinopathy detection needs

appropriate details about certain things, such as symptoms, conditions, and medications. SVM reduces the error rate in the identification process, which maximizes the accuracy rate in the DR detection process [5, 7].

The key contribution of the paper is given as follows:

(i) To accurately diagnose diabetic retinopathy, an efficient DS-KL model is proposed, which incorporates a knowledge learning classifier and pixel-boundary-segmentation technique

(ii) Knowledge learning classifier and delimiting segmentation algorithms are integrated to develop a novel DS-KL algorithm. Our algorithm performs pixel detection at the boundaries and feature optimization in DR classification and labeling of DR in MRI images

(iii) The image features optimization in the DS-KL model by using the delimiting segmentation technique helps to improve the DR diagnostic performance of the DS-KL model for unseen data

(iv) The segmentation performance of the proposed DS-KL model was analyzed with various CNN architectures such as AlexNet, ResNet-50, Inception-v3, VGG-16, and VGG-19

The layout of the paper is organized as follows. Section 2 offers the analysis of the associated literature in diagnosing diabetic retinopathy. Section 3 outlines the holistic explanation of the proposed work's technique. Section 4 gives the implementation setup and outlines the research outcome with a discussion of the results. Section 5 provides the conclusion and recommendations for future investigations.

2. Related Works

Qiao et al. [8] proposed a diabetic retinopathy detection method based on deep learning (DL) algorithm. Microaneurysm symptoms are the early stage of DR that cause vision loss in diabetic patients. Diabetic retinopathy with semantic segmentation method finds the feature of microaneurysm that provides necessary information for the detection process. The proposed method reduces the latency rate in the detection process. The proposed method increases the accuracy rate in the detection process, which improves the performance of the diagnosis process. Karsaz [9] introduced a new CNN-based DR detection method. Support vector domain description (SVDD) is used in CNN to classify the features and patterns of DR. Feature extraction method is used in SVDD that extracts the exact features of DR and produces an optimal set of data for the detection process. SVDD uses a classification process that predicts the critical information which is related to retinopathy. Experimental results show that the proposed CNN method achieves a high accuracy rate in the detection process.

Zago et al. [10] proposed a red lesion localization-based DR detection method. The CNN model is used here to train the data necessary for the detection process. The main aim of the proposed method is to find out the actual cause of DR and to improve the accuracy rate in the detection process. The proposed method reduces both the time and complexity rate in the computation process, which enhances the efficiency of the DR detection process. Gharaibeh [11] introduced a new DR detection method by using the partial swarm optimization (PSO) algorithm. Fundus images provide appropriate DR images that reduce the computation process's latency rate. Fundus images are processed by using an image processing system that finds out the important features of an image. The proposed method achieves a high accuracy rate in the detection process, reducing the error rate in the diagnosis process. Bibi et al. [12] proposed an automated DR detection method based on fundus images. Symptoms and microaneurysms are identified based on fundus images that capture the actual information about DR. Feature extraction process is used here that extracts the important features and patterns from the fundus image. Feature extraction produces an optimal set of data for the DR detection process. The proposed detection method improves the efficiency and performance rate of the diagnosis process.

Guo et al. [13] introduced a Dual-input Attentive RefineNet (DARNet) for multiple lesion segmentation in the DR detection process. The shape, size, texture, and features of DR are first identified by using DARNet. Both decoder and encoder are used in DARNet to extract the information that is available in a dataset or from fundus images. The proposed DARNet method increases the DR detection process's accuracy rate, which improves the system's flexibility and reliability. Hemanth et al. [14] proposed a deep convolutional neural network-based DR detection and classification approach. A digital fundus image produces the required information for the detection process. The proposed method classifies the exact features that are produced by digital fundus images. The proposed method reduces the latency rate in the computation process, enhancing the system's efficiency. Experimental results show that the proposed method achieves a high accuracy rate in the detection process. Hemanth et al. [15] proposed a deep convolutional neural network-based DR detection and classification approach. A digital fundus image produces the required information for the DR detection process. The proposed method classifies the exact features of DR produced by digital fundus images. The proposed method reduces the latency rate in the computation process, which enhances the efficiency of the system. Experimental results show that the proposed method achieves a high accuracy rate in the detection process.

Oh et al. [16] provided a method for the diagnosis of diabetic retinopathy that is based on ultrawide-field fundus imaging and deep learning. In their tests, it is demonstrated that the use of an early treatment diabetic retinopathy study 7-standard field picture generated from ultrawide-field fundus photography achieves statistically superior results than those obtained using images centered on the optic disc and the macula. Katayama et al. [17] developed a powerful framework for semantic segmentation. They integrated three forms of domain adaptation: image-level domain adaptation, interdomain adaptation, and intradomain adaptation. The suggested domain adaption platform can drastically

reduce the amount of time needed to create real-world, photorealistic supervised data. Acharya and Kumar [18] proposed a robust retinal image enhancement approach known as SIAGC for identifying vascular anomalies and assessing the early stages of DR. First, the object of the retinal picture is separated from the backdrop to make the process of detection simpler and more effective. This is carried out to boost the contrast of the retinal images. To prevent excessive augmentation, the plateau limit is implemented in a manner that is distinct to each zone. The overall quality of the image is improved by a mapping function, and an adaptive gamma value was first assessed by using a modified weighted probability density function (PDF). To get the greatest possible improvement in the suggested fitness function, swarm intelligence is employed to make an automated selection of the plateau thresholds and exponentiation parameters used in gamma correction. Abdelsalam and Zahran [19] suggested a novel technique for the early detection of DR based on multifractal geometry. The diagnosis of early nonproliferative diabetic retinopathy which is achieved through an analysis of the macular optical coherence tomography angiography (OCTA) pictures is performed (NPDR), automating the diagnosis process while simultaneously increasing the accuracy of the result by utilizing a supervised machine learning approach such as an SVM algorithm. The accuracy of the categorization approach was 98.5% at this point. This method can also readily distinguish various phases of diabetic retinopathy or other retinal illnesses that impact the arteries or the spread of neovascularization.

Ramasamy et al. [20] created a model for use in DR testing and analysis. In the beginning, we will extract and combine the ophthalmoscopic characteristics from the retina pictures using textural gray-level features such as co-occurrence, run-length matrix, and the coefficients of the Ridgelet Transform. These features will be based on the images of the retina. The sequential minimal optimization (SMO) classification is used to categorize diabetic retinopathy since it considers the characteristics of the retina. The publicly available retinal image datasets are utilized for the performance study, and the trials' results illustrate the suggested technique's quality and efficacy. Fang [21] proposed a pixel-level sample-making approach to PHT identification and built the PHT dataset 2021 (PHTD 2021). This dataset includes 3,000 samples. Second, the DeeplabV3+ model was enhanced to better handle the situation where a text may consist of a lot of words but very little in the way of actual contours. We decreased the number of network layers and the pooling times and raised the convolution kernel and the dilation rate. Using the PHTD 2021 dataset as test data, the enhanced DeeplabV3+ model achieved a 95.06% accuracy in classification. Elsharkawy et al. [22] created a model for use in DR testing and analysis. In the beginning, we will extract and combine the ophthalmoscopic characteristics from the retina pictures using textural gray-level features such as co-occurrence, run-length matrix, and the coefficients of the Ridgelet Transform. These features will be based on the images of the retina. The sequential minimal optimization (SMO) classification categorizes diabetic retinopathy since it considers the characteristics of the retina. The publicly available retinal image datasets are utilized for the performance study, and the results of the trials illustrate the quality and efficacy of the suggested technique.

Islam et al. [23] suggested a method known as supervised contrastive learning (SCL) for the diagnosis of diabetic retinopathy. In this study, the SCL method, which is a two-stage training method with a supervised contrastive loss function, was proposed for the first time to the best of the authors' knowledge to identify the DR and its severity stages from fundus images (FIs) utilizing the "APTOS 2019 Blindness Detection" dataset. The dataset was used to test the accuracy of the SCL method. Experiments were also carried out by using the "Messidor-2" dataset to further validate the performance of the model. To improve the picture quality, CLAHE was used, and a pretrained Xception CNN model was used as the encoder in combination with transfer learning. Yang and Wan [24] mitigated the effect of local noise on segmentation accuracy by introducing a sparse decomposition, and a pixel co-constraint energy functional is constructed to compensate for the fact that individual pixels cannot remember fine-grained information. Furthermore, neighborhood hubs facilitate interaction throughout communities by using a weighted sum of elite solution sets. According to experimental results, the approach has been shown to significantly outperform alternative algorithms in terms of convergence efficiency and accuracy.

Taranum and Rajashekar [25] used image enhancement and deep learning technology to construct an effective image edge weighted linked segmentation model using deep learning (EWLSM-DL) for accurate and rapid identification of diabetic retinopathy to prevent the subsequent retinal damage. In terms of detection precision, the suggested model outperforms the previous techniques. Xing et al. [26] suggested a new structure, the dual attention fusion module (DAFM), to extract accurate dense features for pixel labeling by combining the attention mechanism with the depth pyramid pool module (DPPM). To convert the spatial pyramid structure into output and integrate it with the global pool approach, we create a DPPM. Each decoder layer incorporates the DAFM. As a final step, the low-level and high-level characteristics are combined to provide a unified set of features that may be utilized for semantic segmentation. Our tests and visualizations on the Cityscapes and CamVid datasets demonstrate that the proposed method is successful in real-time semantic segmentation by striking a good compromise between accuracy and speed.

3. Proposed Method

The design goal of DS-KL used for detecting diabetic retinopathy is to reduce hemorrhage kind of risks based on identifying symptoms and processing them through sophisticated clinical procedures. The input DR image is observed from the human eye condition; the detection of DR due to high blood sugar causes diabetes. Having too much sugar in human blood vessels can damage their retina. This

DR detection can cause blindness and vision loss in people with diabetes. Based on DR image processing, the feature can be extracted based on histogram representation, and the symptoms and processing are also identified for reducing the risk factor. In this DR image processing, the segmentation and classification processes are performed through feature extractions that are considered to improve image segmentation. From the knowledge learning, the exudate regions can be classified and detected by using varying histogram representations.

However, to retain the input DR image, the proposed work identifies the changes in histogram representation from which the feature-dependent segmentation process occurred. The different exudate region is observed from multiple inputs based on the training knowledge to improve the segmentation accuracy and precise DR detection. The DR images are required from the people who have high sugar in the blood tissues and are observed at different time intervals that cause diabetes. The objective of this proposed work is to decrease the errors at the time of identifying exudate regions in the input DR images. The challenging task is the segmentation and pixel correlation based on exudate regions. This segmentation process identifies infected and noninfected regions across the delimiting pixel boundaries. From the segmentation process, the newly identified exudate regions are stored in KL to provide training and process pixel correlation. The newly identified exudate regions are stored as records from the previous knowledge-learning instances. The image processing based on diabetic retinopathy and segmentation is processed and identified the infected regions through pixel-boundary-dependent retinopathy. Figure 1 presents the proposed method's process illustration.

In this proposed work, the variation detection is classified as the infected regions and noninfected regions. In an input DR image processing, the feature variations that can be identified from the previous exudate regions are said to be continuous for the next exudate region detection. The process of feature extraction, histogram representation, variation detection, segmentation, and pixel correlation is similar for time and day. Segmentation and pixel correlation processes reduce the chance of error causing. The DR-infected regions are identified as a sequence of the segmentation process. The proposed detection of diabetic retinopathy focuses on such errors through pixel correlation using infected region identification. Initial image processing of DR: let $DR(\text{image})$ represent the input DR image observed from the people at different time intervals such that the feature extraction Fx is given as

$$\left.\begin{array}{l} Fx = DR(\text{image}) - L_{er} * DR(\text{image}) \\ \text{where} \\ arg\min_{t} \sum L_{er}(T) \forall DR(\text{image}) \end{array}\right\}. \tag{1}$$

In (1), the variable L_{er} denotes the limited errors, and the main objective of error minimization for all $DR(\text{image}) \in Fx$ is analyzed. The DR image processing is based on two instances, namely, histogram representation (h_r) and variation detection (v_d) with different exudate regions. Therefore, $\text{image}^p = h_r + v_d$ such that the variation detection is observed from each instance of histogram changes identification and vice versa. If n illustrates the input images, then $v_d = \{(n * \text{image}^p) - (h_r + v_d)\}$ is the continuous analysis of diabetic retinopathy to be detected from the DR images, where $D^S(h_r, v_d)$ and $D^S(v_d)$ represent the delimiting segmentation of exudate regions detected in n intervals and L_{er} is identified in all variation detection process such that

$$D^S(h_r, v_d) = n * (h_r + v_d) + DR(\text{image}), L_{er} = 0. \tag{2}$$

Also,

$$D^S(v_d) = \left(\frac{L_{er}}{n} * v_d\right) + [L_{er} * DR(\text{image})], L_{er} \neq 0. \tag{3}$$

Based on (2) and (3), the exudate region is observed based on $\{n * (h_r + v_d)\}$ and $(L_{er}/n * v_d)$ condition relies on training knowledge from different input instances with $DR(\text{image})$. Now, the exudate region Ex_r detection is given as

$$Ex_r = D^S(h_r, v_d) - D^S(v_d) \approx n * (h_r + v_d) - \left(\frac{L_{er}}{n} * v_d\right) + [L_{er}.DR(\text{image})]. \tag{4}$$

In (4), the instance of $v_d \in \text{image}^p$ is to be computed previously for addressing the first variation detection based on histogram changes as in (5). This assessment is used to identify errors based on the segmentation process using knowledge learning. The segmentation process is illustrated in Figure 2.

The histogram representations are classified as fixed and varying based on their representation. The bounding/overlapping regions are detected for Ex_r. This is used for pixel identification and delimiting segment classification, as shown in Figure 2. The image segmentation process is performed using the feature variation mitigated through continuous knowledge learning. From this segmentation of multiple inputs, the sequence of $n \in v_d$ is estimated as

$$n(v_d) = \sum_{i=1}^{T} \frac{(1 - h_r + v_d)^{n-1} v_{d-1}}{n}. \tag{5}$$

In (5), the instance of the previous exudate region is v_{d-1} and the delimiting pixel boundaries instance based on the conditions $(h_r + v_d)$ and $\sum_{i=1}^{T} (1 - h_r + v_d)^{n-1} v_{d-1}/n$. Therefore, the segmentation process identifies DR-defected and nondefected regions from the delimiting pixel boundaries in the above sequence, $Fx = \text{image}^p(h_r, v_d) - [1 - n(\text{image}^p(v_d))]$ is the final solution for segmentation with $L_{er} \neq 0$. The feature variation analysis based on exudate regions in image processing improves the segmentation accuracy through knowledge learning. The pixel correlation of (Pc_{h_r, v_d}) and (Pc_{v_d}) for region detection and training instances at the initial DR image processing is computed as

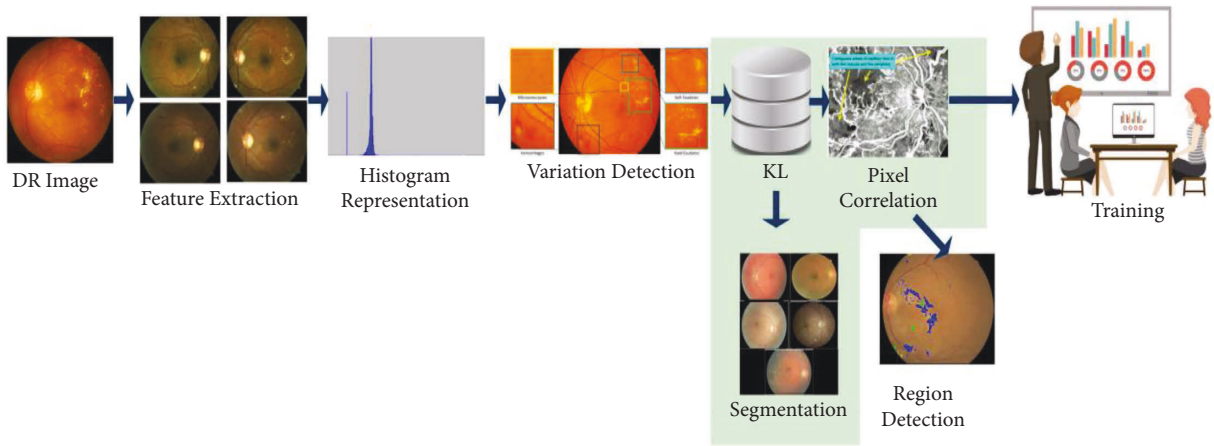

Figure 1: An illustration of the proposed method.

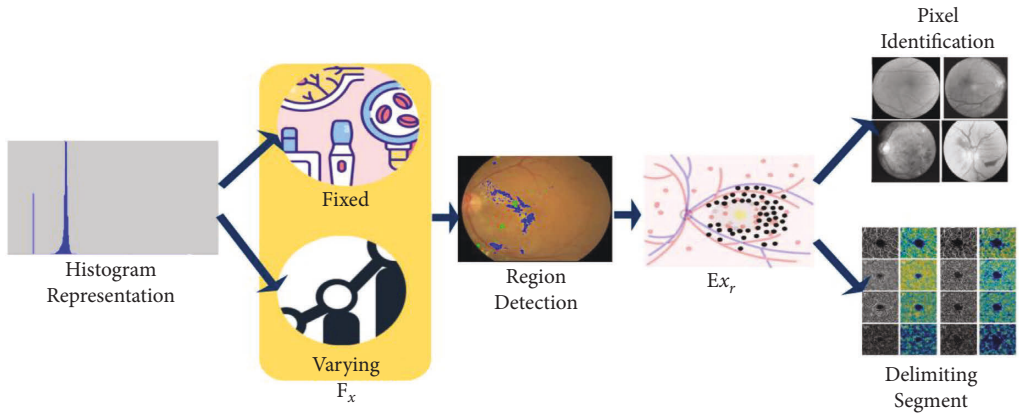

Figure 2: Illustrative example of the segmentation process.

$$\left(Pc_{h_r,v_d}\right) \simeq \frac{\text{image}^p\left(h_r.v_d\right) * T}{\sum_{n\in T}\left[DR\left(\text{image}\right)\right]_n}, \tag{6}$$

where the knowledge learning stores the newly identified exudate region for training and pixel correlation based on the fault region detection during DR image processing and infected region identification Inf_r through KL is computed as

$$Inf_r \simeq \frac{\text{image}^p\left(h_r.v_d\right) * Pc}{\sum_{n\in T}\left(n + h_r.v_d\right)_n\left[1 - n\left(v_d\right)\right]_n}. \tag{7}$$

(6) and (7) are used to compute the segmentation and pixel correlation process based on the exudate region detection in histogram representation and variation detection from the DR image input at different time intervals T. Figure 3 presents the correlation process using the KL.

The Ex_r is pixelated for correlation with $n(v_d)$. This is performed using the knowledge learned for $D^s\left(h_r, v_d\right)$ and $D^s\left(v_d\right)$ independently. Based on the unidentified region (error), the training for $D^s\left(v_d\right)\forall\left(P_{ch_r}, v_d\right)$ is performed. This is recurrent until $\max\left\{\inf_r\right\}$ is identified $\forall Fx$ (refer to Figure 3). The KL stores the newly identified exudate region from the previous region detection. The continuous process of image segmentation assists in finding the infected region from the input image and error detection based on pixel correlation and training instance. Segmentation and correlation with region detection and error in variation detection are finally detected, and the infected and noninfected regions are also observed. If any fault region is observed during pixel correlation, that recurrent training is provided to improve the segmentation in input DR images. The consecutive manner of image processing reduces error and increases the segmentation accuracy and precise detection of exudate regions through computer-aided clinical procedures.

4. Implementation and Discussion

The proposed method was applied using the widely used public DIARETDB1 [27] retinopathy dataset and Indian Diabetic Retinopathy Image Dataset (IDRiD) [28]. DIARETDB1 is comprised of 89 fundus pictures with 5 healthy samples and the rest samples having mild diabetic retinopathy symptoms, including hemorrhages, microaneurysms, hard exudates, and soft exudates. This dataset was utilized for the identification of hard exudate. IDRiD is

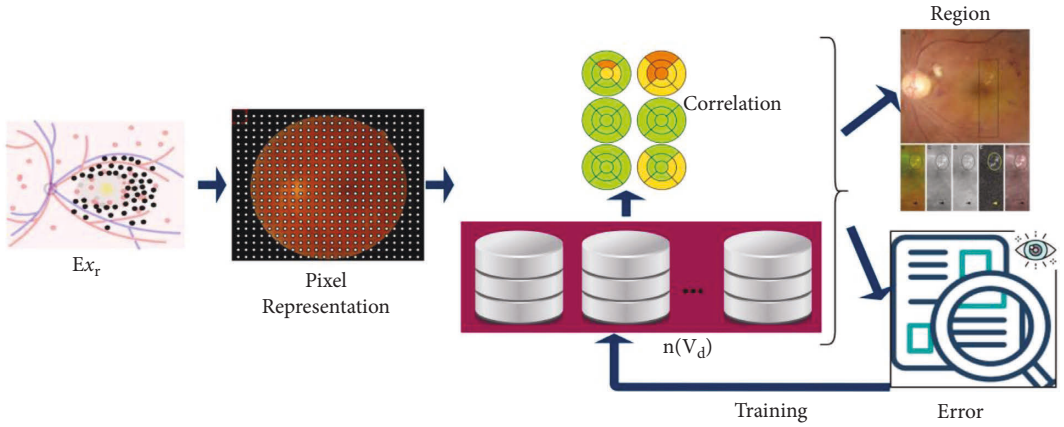

Figure 3: Correlation process by using KL.

the first dataset that has both conventional diabetic retinopathy lesions and normal retinal features identified at the pixel level. Each picture in this collection has associated information about the level of diabetic retinopathy and diabetic macular edema present. Because of this, it is ideal for testing and refining image processing techniques for diabetic retinopathy screening. In addition to general performance accuracy, several performance indicators were investigated for the suggested method. These metrics are similarity measurements based on pixel-to-pixel template matching between the ground-truth template and its counterpart derived by the suggested approach. Correct categorization requires the definition of true positive (TP) and true negative (TN). TP specifies the number of candidate pixels that have been successfully recognized as candidates, whereas TN specifies the number of noncandidate pixels that have been correctly identified as noncandidate pixels. False positive (FP) and false negative (FN) are specified for misclassification. FP is the misclassification of a noncandidate pixel as a candidate pixel, whereas FN is the misclassification of a candidate pixel as a noncandidate. The proposed similarity metrics are defined in equations (8)–(13).

$$\text{Accurcay} = \frac{\text{TP} + \text{TN}}{\text{TP} + \text{TN} + \text{FP} + \text{FN}}, \tag{8}$$

$$\text{Precision} = \frac{\text{TP}}{\text{TP} + \text{FP}}, \tag{9}$$

$$\text{Sensitivity} = \frac{\text{TP}}{\text{TP} + \text{FN}}, \tag{10}$$

$$\text{Specificity} = \frac{\text{TN}}{\text{TN} + \text{FP}}, \tag{11}$$

$$MCC = \frac{\text{TP} \times \text{TN} - \text{FP} \times \text{FN}}{\sqrt{(\text{TP} + \text{FP})(\text{TP} + \text{FN})(\text{TN} + \text{FP})(\text{TN} + \text{FN})}}, \tag{12}$$

$$\text{Dicecoefficient} = \frac{2\text{TP}}{2\text{TP} + \text{FP} + \text{FN}}. \tag{13}$$

The proposed method is validated using accuracy, precision, and error metrics for varying features and classifications. The DR images from [27] are used for detection and classification; we added 180 detected images and 512 training inputs. The methods AD-FF [12] and PSO-GIT2FMFs [11] are considered alongside the proposed DS-KL method in the metrics comparison.

In Figure 4, the early and precise detection of diabetic retinopathy through histogram representation based on feature extraction and variations is used for identifying DR-affected regions. Figure 5 depicts the accuracy analysis of diabetic retinopathy classification through feature extraction. The image processing is to improve the segmentation accuracy based on histogram changes during pixel correlation, not delaminating pixel boundaries by using knowledge learning. Therefore, the error is identified in the exudate region process, preventing high accuracy due to changes in the histogram for image segmentation.

The feature extraction and histogram representation are based on the detection of DR for individuals in the

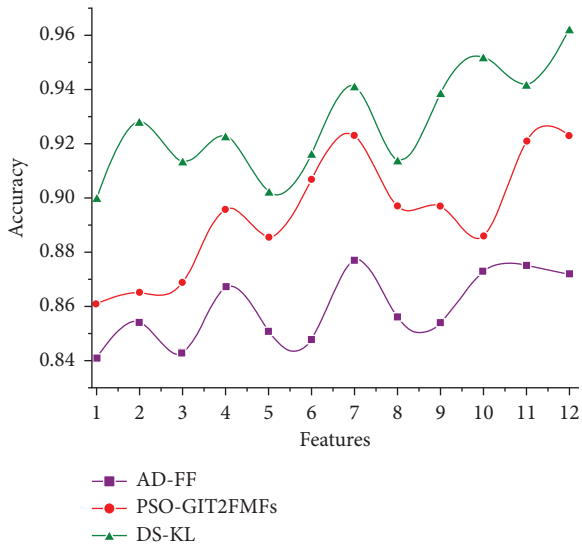

Figure 4: Feature accuracy analysis.

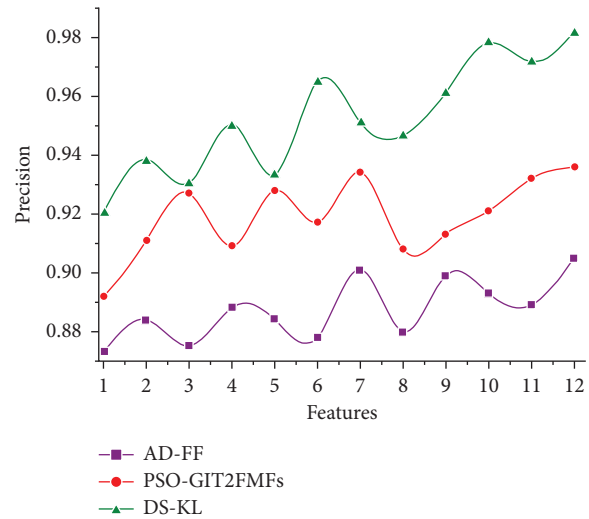

Figure 6: Feature detection precision analysis.

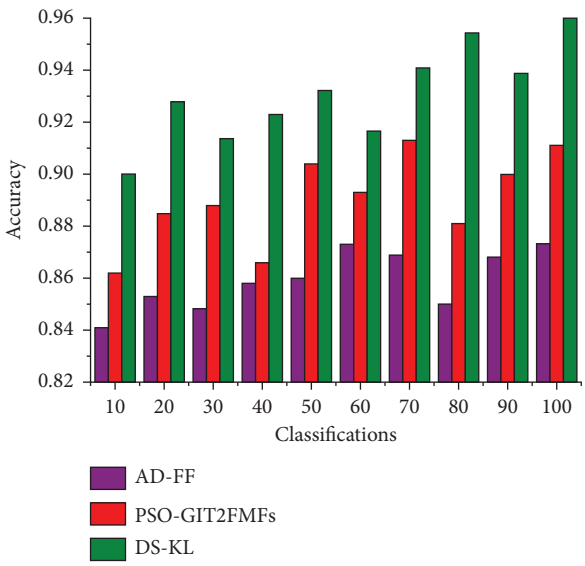

Figure 5: Classification accuracy analysis.

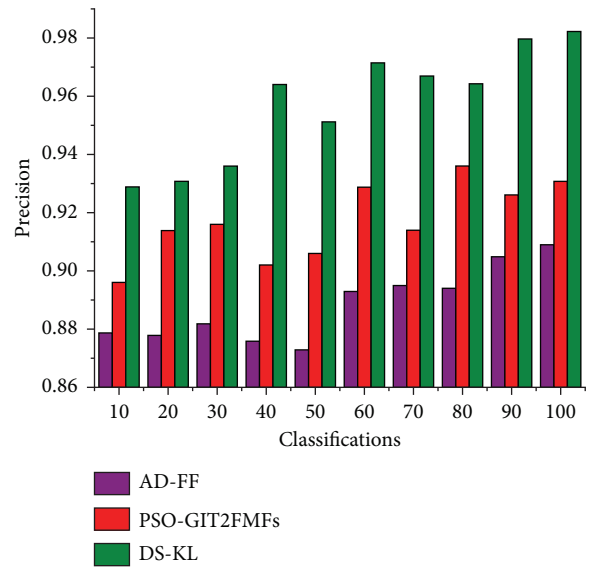

Figure 7: Classification precision analysis.

healthcare system as the first instance observed from the people. The classification and detection of exudate regions by using varying histograms are analyzed to reduce the error occurrence based on the segmentation, as represented in Figures 6 and 7. This proposed method satisfies high segmentation accuracy by image processing. Therefore, the changes in histogram representation are addressed for maximizing the pixel correlation for training the current knowledge based on the variation detection which is high precision for identifying infected regions.

In this proposed work, DR-infected and noninfected region detection through histogram representation does not verify pixel correlation for exudate regions at the time of image processing. The addressing of the DR-infected region based on feature variation analysis is computed from identifying symptoms and processing by using clinical procedures for knowledge learning at different time intervals. In this proposed work, the exudate region detection is used for identifying DR-affected peoples and achieves less error, as illustrated in Figures 8 and 9.

DR-affected areas are identified by the early and accurate diagnosis of diabetic retinopathy by using histogram representation based on feature extraction and changes. Figures 10 and 11 display the sensitivity analysis of diabetic retinopathy using feature extraction. The sensitivity analysis aims to measure the performance of feature selection and classification with the proposed DR model.

Figures 12 and 13 depict the specificity analysis for feature selection and DR classification. DS-KL is proposed for identifying and recognizing exudate zones utilizing different histograms. Based on the input image's histogram changes, a process of feature-dependent segmentation is carried out. Specificity analysis shows the detection of

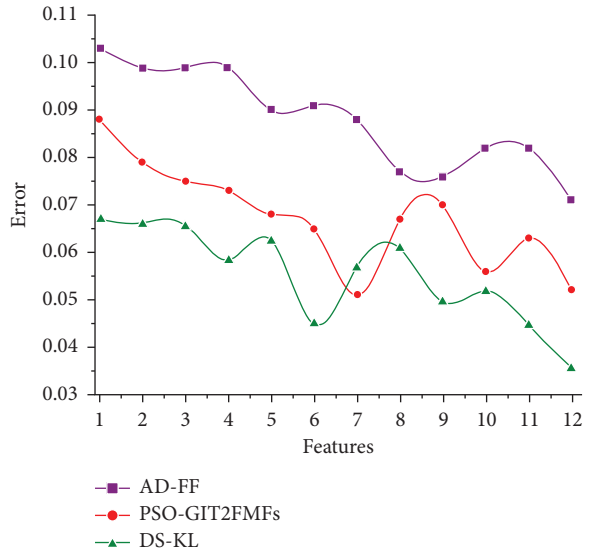

Figure 8: Error rate in feature selection.

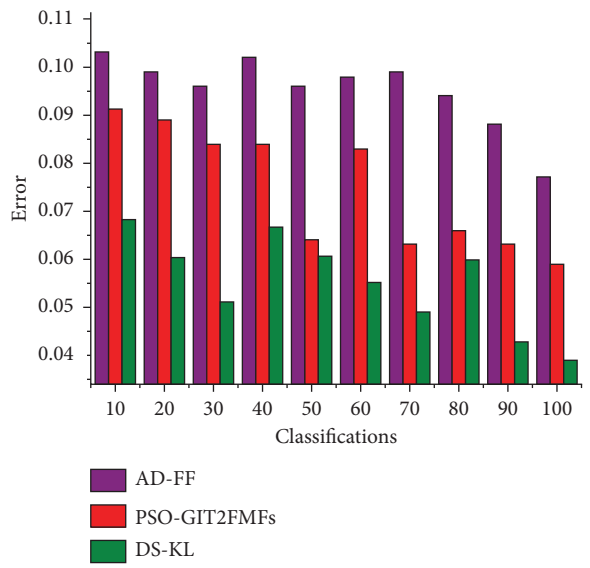

Figure 9: Error analysis in classification of DR.

irrelevant features and improper classification correctly. This process distinguishes between infected and uninfected areas based on pixel boundaries.

Figures 14 and 15 illustrate the Matthews correlation coefficient (MCC) performance analysis with respect to feature selection and DR classification. MCC is analyzed to better understand the error matrix components (TP, TN, FP, and FN) for efficient evaluation of DR class predictions. The above results are summarized in Tables 1 and 2 for the varying features and classifications, respectively.

The assessment metrics and visualization of auto segmentation in the testing dataset demonstrate that the proposed method can diagnose and segment the exudate region in DR images. Similar to the segmentation of DR images, we can confirm that pixel accuracy is not an acceptable assessment metric for semantic segmentation in the presence

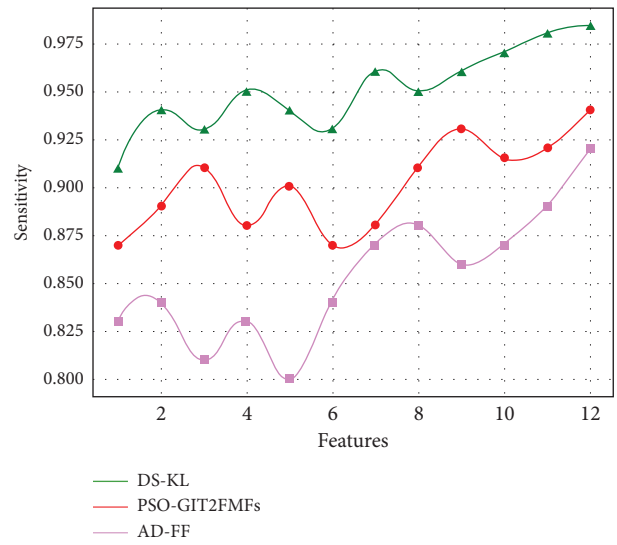

Figure 10: Sensitivity analysis in feature selection.

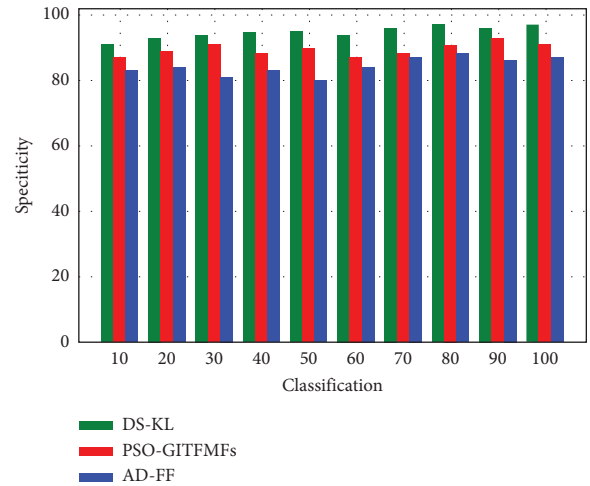

Figure 11: Sensitivity analysis in DR classification.

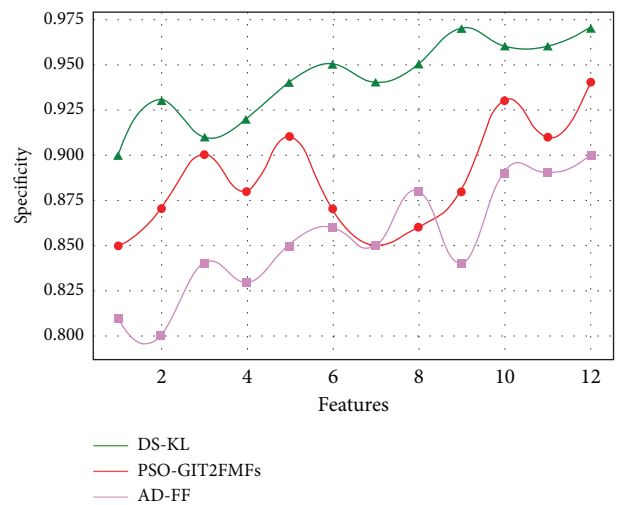

Figure 12: Specificity analysis in feature selection.

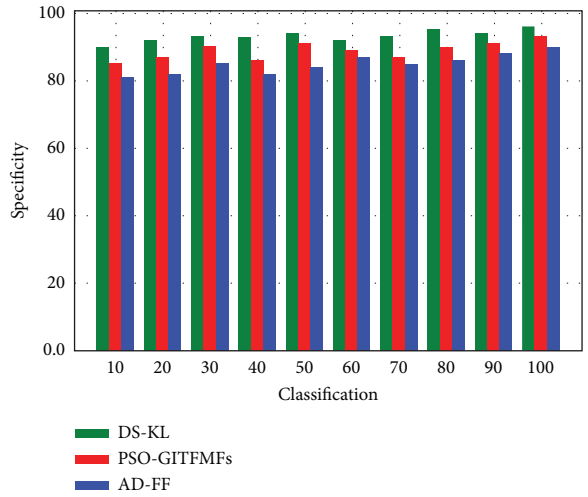

Figure 13: Specificity analysis in DR classification.

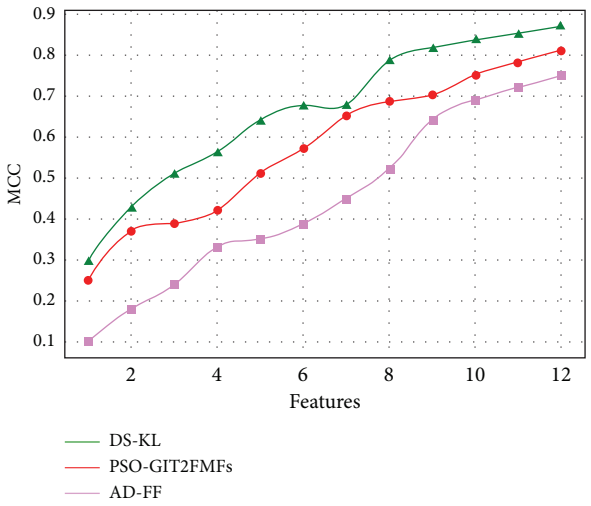

Figure 14: MCC analysis of feature selection.

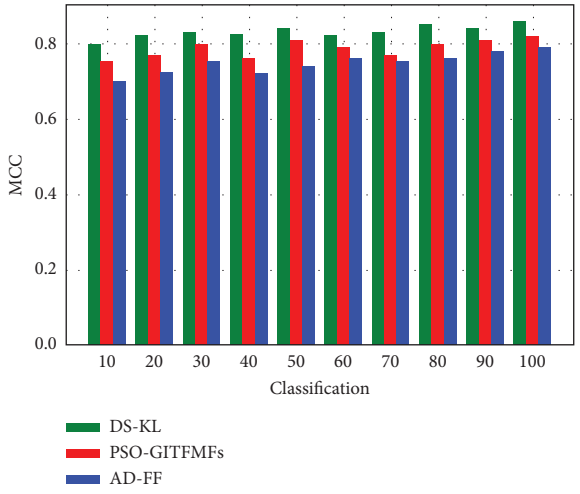

Figure 15: MCC analysis of DR classification.

Table 1: Analysis summary of features.

Metrics	AD-FF	PSO-GIT2FMFs	DS-KL	Proposed improvements
Accuracy	0.872	0.923	0.9623	6.48% high
Precision	0.905	0.936	0.982	6.15% high
Error	0.071	0.052	0.0357	7.74% less
Sensitivity	0.915	0.954	0.989	7.4% high
Specificity	0.902	0.941	0.974	7.2% high
MCC	0.786	0.813	0.877	9.1% high

Table 2: Analysis summary for classifications.

Metrics	AD-FF	PSO-GIT2FMFs	DS-KL	Proposed improvements
Accuracy	0.873	0.911	0.9651	7.31% high
Precision	0.909	0.931	0.9824	6.24% high
Error	0.077	0.059	0.0389	8.73% less
Sensitivity	0.874	0.916	0.953	7.9% high
Specificity	0.891	0.946	0.976	8.5% high
MCC	0.793	0.816	0.852	5.9% high

of class imbalance because the backdrop is the dominating class in ground-truth photos. In addition, high pixel precision might be deceiving in certain computer vision applications.

The results in Table 3 elucidate the accuracy, precision value, sensitivity, and specificity of the proposed DS-KL segmentation in the IDRiD dataset. The proposed method outperformed all other existing image segmentation techniques with an accuracy of 97.67%, dice coefficient value of 98.45%, sensitivity value of 98.65%, and specificity value of 99.76%.

Next, the proposed DL-KS segmentation technique is combined with several CNN architectures including AlexNet [29], Inception-v3 [30], ResNet-50 [29], VGG-16 [31] and VGG-19 [32]. Figure 16 displays the classification accuracy of CNN architectures aided with DL-KS segmentation applied to the IDRiD dataset. It is clear that the greatest

Table 3: Comparative performance of the published technique and the proposed method with IDRiD dataset.

Metrics	Lesion localization [10]	Attentive RefineNet [14]	Multifractal geometry [19]	Ridgelet features [20]	Proposed DS-KL
Accuracy	0.912	0.9217	0.985	0.910	0.9767
Dice value	0.821	0.813	0.868	0.890	0.9245
Sensitivity	0.940	0.8936	0.960	0.909	0.9865
Specificity	0.959	0.9328	0.973	0.910	0.9976

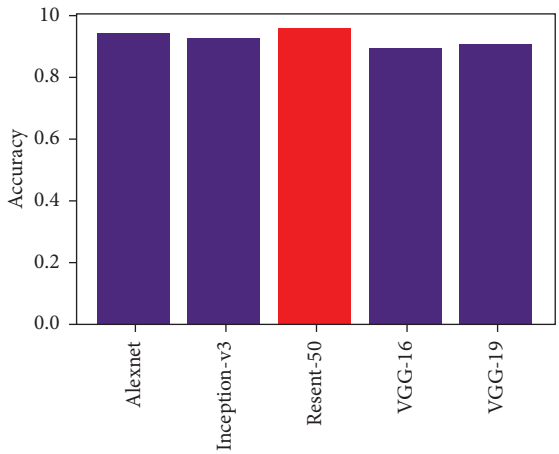

Figure 16: Accuracy of CNN architectures.

Table 4: Comparative performance of the proposed DS-KL technique using different datasets.

Metrics	DIARETDB1	IDRiD	Kaggle	Messidor	DDR
Accuracy	0.9623	0.9767	0.9814	0.9532	0.9791
Dice coefficient	0.852	0.9245	0.9459	0.9019	0.9523
Sensitivity	0.953	0.9865	0.9963	0.9345	0.9815
Specificity	0.976	0.9976	0.9987	0.9578	0.9873

classification accuracy of individual CNN architectures, such as AlexNet, Inception-v3, ResNet-50, VGG-16, and VGG-19, respectively, on the IDRiD dataset, is obtained as 95.60%, 93.60%, 96.20%, 91.09%, and 93.20%. When applying the proposed data partition strategy, the classification accuracy of the various CNN architectures is maximized. It is noted that the suggested DS-KL method improves upon the individual CNN designs in terms of classification accuracy for detecting retinal exudates.

Three other datasets, such as Kaggle [33], Messidor [34], and DDR [35], are also used as the testbed for analyzing the performance of the proposed DS-KL segmentation technique. Table 4 displays the outcomes of the proposed DS-KL segmentation from the DR screening experiment by using various datasets. Our findings imply that our technique, if employed in a real scenario for DR screening, can greatly decrease the load on specialists and improve the accuracy of DR detection.

From our research, we conclude that CNNs have been used for the evaluation of fundus images for the diagnosis of DR, with shown success in segmentation and localization tasks. Damage to the DR is a potentially blinding complication of diabetes. However, the diagnosis of erroneous symptoms in fundoscopy relies on various complex features and their distributions within the image. CNN's successive layers gradually extract the most distinguishable elements, resulting in an increasingly larger input image size. The state-of-the-art procedure in our proposed DS-KL segmentation improved the accuracy of DR screening. Though deep learning-based DR detection studies consistently show outstanding accuracy in severe instances, moderate case detection remains challenging. This limitation prevents the widespread deployment of automated mass screening, which may lead to the emergence of more complicated conditions in the future due to the likely absence of the early phase of DR.

5. Conclusion

This article disclosed a novel delimiting segmentation method using knowledge learning to improve DR detection accuracy. The proposed method relies on histogram variation classification for identifying exudate regions. The feature extraction from the specific regions improves the segmentation based on knowledge classifications. Previous delimiting pixels and boundaries are included in the classification process to improve the segmentation. Based on the identified regions, the knowledge base is updated with the pixel correlation output for retaining the DR detection precision. This update and correlation are recurrent until maximum detection is facilitated through classification. The experimental analysis shows that the proposed method improves accuracy by 6.48% and precision by 6.15% and reduces error by 7.74% for the varying features. The experimental analysis shows that the proposed method improves accuracy by 6.48%, precision by 6.15%, specificity by 7.8%, sensitivity by 7.65%, and MCC by 7.5% and reduces error by 7.74% for the varying features. Moreover, the proposed segmentation model is analyzed with various datasets, such as IDRiD, DIARETDB1, Kaggle, Messidor, and DDR, utilizing different CNN architectures. In the future, we will analyze a prospective improvement and extension of the proposed DS-KL segmentation to enable classification and prediction of the presence and extent of DR by using multichannel 3D MRI volumes.

Data Availability

The data used to support the findings of this study are available from the authors upon request.

Conflicts of Interest

The authors declare that they have no conflicts of interest.

References

[1] Y. Zhou, B. Wang, L. Huang, S. Cui, and L. Shao, "A benchmark for studying diabetic retinopathy: segmentation, grading, and transferability," *IEEE Transactions on Medical Imaging*, vol. 40, no. 3, pp. 818–828, 2020.

[2] J. Xue, S. Yan, J. Qu et al., "Deep membrane systems for multitask segmentation in diabetic retinopathy," *Knowledge-Based Systems*, vol. 183, Article ID 104887, 2019.

[3] A. Skouta, A. Elmoufidi, S. Jai-Andaloussi, and O. Ouchetto, "Hemorrhage semantic segmentation in fundus images for the diagnosis of diabetic retinopathy by using a convolutional neural network," *Journal of Big Data*, vol. 9, no. 1, pp. 1–24, 2022.

[4] E. O. Rodrigues, A. Conci, and P. Liatsis, "Element: multi-modal retinal vessel segmentation based on a coupled region growing and machine learning approach," *IEEE Journal of Biomedical and Health Informatics*, vol. 24, no. 12, pp. 3507–3519, 2020.

[5] M. Toğaçar, "Detection of retinopathy disease using morphological gradient and segmentation approaches in fundus images," *Computer Methods and Programs in Biomedicine*, vol. 214, Article ID 106579, 2022.

[6] Q. Li, S. Fan, and C. Chen, "An intelligent segmentation and diagnosis method for diabetic retinopathy based on improved U-NET network," *Journal of Medical Systems*, vol. 43, no. 9, pp. 1–9, 2019.

[7] Y. Guo and Y. Peng, "CARNet: cascade attentive RefineNet for multi-lesion segmentation of diabetic retinopathy images," *Complex & Intelligent Systems*, vol. 8, no. 2, pp. 1681–1701, 2022.

[8] L. Qiao, Y. Zhu, and H. Zhou, "Diabetic retinopathy detection using prognosis of microaneurysm and early diagnosis system for non-proliferative diabetic retinopathy based on deep learning algorithms," *IEEE Access*, vol. 8, Article ID 104292, 2020.

[9] A. Karsaz, "A modified convolutional neural network architecture for diabetic retinopathy screening using SVDD," *Applied Soft Computing*, vol. 125, Article ID 109102, 2022.

[10] G. T. Zago, R. V. Andreão, B. Dorizzi, and E. O. T. Salles, "Diabetic retinopathy detection using red lesion localization and convolutional neural networks," *Computers in Biology and Medicine*, vol. 116, Article ID 103537, 2020.

[11] N. Y. Gharaibeh, "Detection of diabetic retinopathy using partial swarm optimization (PSO) and Gaussian interval type-2 fuzzy membership functions (GIT2FMFS)," *Materials Today Proceedings*, 2020.

[12] I. Bibi, J. Mir, and G. Raja, "Automated detection of diabetic retinopathy in fundus images using fused features," *Physical and Engineering Sciences in Medicine*, vol. 43, no. 4, pp. 1253–1264, 2020.

[13] S. Goel, S. Gupta, A. Panwar et al., "Deep learning approach for stages of severity classification in diabetic retinopathy using color fundus retinal images," *Mathematical Problems in Engineering*, vol. 2021, Article ID 7627566, 8 pages, 2021.

[14] Y. Guo and Y. Peng, "Multiple lesion segmentation in diabetic retinopathy with dual-input attentive RefineNet," *Applied Intelligence*, vol. 52, pp. 1–25, 2022.

[15] D. J. Hemanth, O. Deperlioglu, and U. Kose, "An enhanced diabetic retinopathy detection and classification approach using deep convolutional neural network," *Neural Computing & Applications*, vol. 32, no. 3, pp. 707–721, 2020.

[16] K. Oh, H. M. Kang, D. Leem, H. Lee, K. Y. Seo, and S. Yoon, "Early detection of diabetic retinopathy based on deep learning and ultra-wide-field fundus images," *Scientific Reports*, vol. 11, no. 1, pp. 1–9, 2021.

[17] T. Katayama, T. Song, X. Jiang, J. S. Leu, and T. Shimamoto, "Domain adaptation through photorealistic enhanced images for semantic segmentation," *Mathematical Problems in Engineering*, vol. 2022, Article ID 1848857, 12 pages, 2022.

[18] U. K. Acharya and S. Kumar, "Swarm intelligence based adaptive gamma corrected (SIAGC) retinal image enhancement technique for early detection of Diabetic Retinopathy," *Optik*, vol. 247, Article ID 167904, 2021.

[19] M. M. Abdelsalam and M. A. Zahran, "A novel approach of diabetic retinopathy early detection based on multifractal geometry analysis for OCTA macular images using support vector machine," *IEEE Access*, vol. 9, Article ID 22844, 2021.

[20] L. K. Ramasamy, S. G. Padinjappurathu, S. Kadry, and R. Damaševičius, "Detection of diabetic retinopathy using a fusion of textural and ridgelet features of retinal images and sequential minimal optimization classifier," *PeerJ Computer Science*, vol. 7, p. e456, 2021.

[21] H. Fang, "Semantic segmentation of PHT based on improved DeeplabV3+," *Mathematical Problems in Engineering*, vol. 2022, Article ID 6228532, 8 pages, 2022.

[22] M. Elsharkawy, A. Sharafeldeen, A. Soliman et al., "A novel computer-aided diagnostic system for early detection of diabetic retinopathy using 3D-OCT higher-order spatial appearance model," *Diagnostics*, vol. 12, no. 2, p. 461, 2022.

[23] M. R. Islam, L. F. Abdulrazak, M. Nahiduzzaman et al., "Applying supervised contrastive learning for the detection of diabetic retinopathy and its severity levels from fundus images," *Computers in Biology and Medicine*, vol. 146, Article ID 105602, 2022.

[24] Z. Yang and J. Wan, "A threshold segmentation algorithm for sculpture images based on sparse decomposition," *Mathematical Problems in Engineering*, vol. 2022, Article ID 8523370, 8 pages, 2022.

[25] M. P. L. Taranum and J. S. Rajashekar, "Image based Edge weighted linked segmentation model using deep learning for detection of diabetic retinopathy," *Traitement du Signal*, vol. 39, no. 1, 2022.

[26] Y. Xing, L. Zhong, and X. Zhong, "DARSegNet: a real-time semantic segmentation method based on dual attention fusion Module and encoder-decoder network," *Mathematical Problems in Engineering*, vol. 2022, Article ID 6195148, 10 pages, 2022.

[27] Diaretdb1, "Standard diabetic retinopathy database," 2009, http://www2.it.lut.fi/project/imageret/diaretdb1/.

[28] P. Porwal, S. Pachade, R. Kamble et al., "Diabetic retinopathy: segmentation and grading challenge workshop at IEEE international symposium on biomedical imaging," 2018, https://ieee-dataport.org/open-access/indian-diabetic-retinopathy-image-dataset-idrid.

[29] R. E. Hacisoftaoglu, M. Karakaya, and A. B. Sallam, "Deep learning frameworks for diabetic retinopathy detection with smartphone-based retinal imaging systems," *Pattern Recognition Letters*, vol. 135, pp. 409–417, 2020.

[30] C. Bhardwaj, S. Jain, and M. Sood, "Diabetic retinopathy severity grading employing quadrant-based Inception-V3 convolution neural network architecture," *International Journal of Imaging Systems and Technology*, vol. 31, no. 2, pp. 592–608, 2021.

[31] S. Albahli and G. N. Ahmad Hassan Yar, "Automated detection of diabetic retinopathy using custom convolutional neural network," *Journal of X-Ray Science and Technology*, vol. 30, pp. 1–17, 2022.

[32] N. M. Al, M. Al-Moosawi, and R. S. Khudeyer, "ResNet-34/DR: a residual convolutional neural network for the diagnosis of diabetic retinopathy," *Informatica*, vol. 45, no. 7, 2021.

[33] kaggle, "Diabetic retinopathy dataset," 2015, https://www.kaggle.com/c/diabetic-retinopathy-detection/data.

[34] E. Decencière, X. Zhang, G. Cazuguel et al., "Feedback on a publicly distributed image database: the Messidor database," *Image Analysis and Stereology*, vol. 33, no. 3, pp. 231–234, 2014.

[35] T. Li, Y. Gao, K. Wang, S. Guo, H. Liu, and H. Kang, "Diagnostic assessment of deep learning algorithms for diabetic retinopathy screening," *Information Sciences*, vol. 501, pp. 511–522, 2019.